

Gaussian Process-based calculation of look-elsewhere trials factor

V. Ananiev¹ and A. L. Read^{1*}[†]

¹Department of Physics, University of Oslo, Boks 1072 Blindern, Oslo, NO-0316, Norway.

*Corresponding author(s). E-mail(s): a.l.read@fys.uio.no;

Contributing authors: viktor.ananiev@fys.uio.no;

[†]These authors contributed equally to this work.

Abstract

In high-energy physics it is a recurring challenge to efficiently and precisely (enough) calculate the global significance of, e.g., a potential new resonance. The Gross and Vitells trials factor approximation [1] and [2], which is based on the average expected “up-crossings” of the significance in the search region, has revolutionized this for significances above 3 standard deviations, but the challenges of actually calculating the average expected up-crossings and the validity of the approximation for smaller significances remain. We propose a new method that models the significance in the search region as a Gaussian Process (GP). The covariance matrix of the GP is calculated with a carefully designed set of Asimov background-only data sets, comparable in number to the random background-only data sets used in a typical analysis, however, the average up-crossings (and even directly the trials factor for both low and moderate significances) can subsequently be calculated to the desired precision with a computationally inexpensive random sampling of the GP. Once the covariance of the GP is determined, the average number of up-crossings can be computed analytically. In our work we give some highlights of the analytic calculation and also discuss some peculiarities of the trials factor estimation on a finite grid. We illustrate the method with studies of three complementary statistical models, including the one studied by Gross and Vitells [1].

Keywords: Resonance search, Statistical significance, Look-elsewhere effect, Trials factor, Gaussian process

1 Introduction

In a typical search for a new particle or resonance in a high-energy physics experiment, the statistical model consists of a relatively narrow signal peak on top of a broad background in the invariant mass spectrum. In general, the location of the signal is not known *a priori* so the likelihood is maximized for signal masses and amplitudes in the “search region” of mass. In some models the

width of the signal is not uniquely specified, leading to a 2-dimensional search region. The background model has typically one or more nuisance parameters that describe the form and normalization of the background distribution. The signal parameters such as width and mass, however, are not defined under the background hypothesis. In this case, the significance at the location of maximum likelihood of the signal plus background hypothesis (local significance) should be reduced to account for random fluctuations of the background that can occur anywhere in the

search region. The corrected significance is called “global significance”, and the ratio between the corresponding global and local p-values or tail probabilities, which is a function of the observed local significance, is called the “trials factor”. The whole situation is often referred to in high energy physics as the “look-elsewhere effect”.

The most straightforward way to estimate the trials factor is to analyse a large ensemble of Monte Carlo data sets (toy data sets or “toys”) generated from the background model and to count how many times the significance exceeds a local significance level. However, Monte Carlo toys are usually expensive to analyse in terms of computational resources.

Gross and Vitells, in their studies of the look-elsewhere effect [1, 2], suggested a way to estimate the trials factor for large local significances $\gtrsim 3\sigma$. Their approach sets the upper bound to the trials factor based on the average Euler characteristic of the χ^2 field, a field that emerges from the signal nuisance parameter scan. In the one-dimensional case the average Euler characteristic can be estimated from the average number of up-crossings counted at some reference level of local significance and then propagated to higher levels. This method, however, can be very conservative when applied to lower significances.

We focus on models with a test statistic that follows a χ^2 distribution with 1 degree of freedom. This allows us to turn the χ^2 field into a significance field that we then propose in Sec. 2 to approximate with a Gaussian Process whose covariance matrix is calculated with a set of Asimov data sets. The resulting GP allows us to efficiently sample approximate Monte Carlo toys and, therefore, to quickly evaluate the trials factor via an approximate brute force method.

As described in Sec. 2.1, once the covariance of the GP is determined, the average number of up-crossings can, in fact, be computed analytically. We also discuss some peculiarities of the trials factor estimation on a finite grid in Sec 2.2.

We demonstrate our method applied to the background template model used by Gross and Vitells in their study (Sec. 3.1) as well as exponential background models with 1-dimensional (Sec. 3.2) and 2-dimensional (Sec. 3.3) search regions inspired by searches for a resonance due to

$H \rightarrow \gamma\gamma$ decays in proton-proton collisions at the Large Hadron Collider [3, 4].

2 Method

In resonance searches the signal model has a nuisance parameter M that is not present under the background-only hypothesis and that denotes the set of points that constitute the search region. The search region itself may be one-dimensional, for a case when the mass of a hypothetical particle is unknown, or many dimensional, for example 2-dimensional, when the decay width is also not specified uniquely. We elaborate on the 2-D search region in Sec. 3.3.

We focus on the case where the signal model has 1 free parameter (e.g. signal amplitude or strength μ) for each point in M , therefore the profile likelihood test statistic

$$t(M) = -2 \ln \lambda(M), \quad \lambda(M) = \frac{\mathcal{L}(0, \hat{\theta})}{\mathcal{L}(\hat{\mu}, M, \hat{\theta})} \quad (1)$$

follows a χ^2 distribution with 1 degree of freedom. Here θ is one or more additional nuisance parameters that maximize the likelihood under the background ($\hat{\theta}$) or signal plus background ($\hat{\theta}$) hypotheses. We then construct the significance $Z(M)$ as follows:

$$Z(M) = \sqrt{t(M)} \operatorname{sign} \hat{\mu}. \quad (2)$$

According to Cowan et al. [5, Eq. 17], Z follows a Gaussian distribution. Moreover, since we are interested in the trials factor under the background hypothesis $H_0 : \mu = 0$, the best-fit signal strength $\hat{\mu}$ is distributed as a standard normal distribution $\mathcal{N}(0, 1)$. To compute the trials factor we need to determine the probability that $Z(M)$ exceeds the local significance observed in the data for any M in the search region.

We propose to approximate the ensemble of curves $Z(M)$ with a family of samples from some Gaussian Process. Such an approximation increases the performance of the sampling without introducing significant bias. Properties of Z -curves (significance curves) are reflected in the GP mean, that should be set to 0, and the kernel K with $K(M_i, M_i) = 1$, i.e., the kernel must have 1 on the diagonal.

The crucial step of our proposal is to estimate $\hat{\Sigma}$, which is the covariance matrix of the GP evaluated on the grid specific to the problem. Properties of the kernel K , and subsequently of the covariance matrix of the GP, $\hat{\Sigma}$, can be formally expressed as follows:

$$\begin{aligned}\hat{\Sigma}_{ij} &= \text{cov}[Z(M_i), Z(M_j)], \\ \hat{\Sigma}_{ii} &= 1.\end{aligned}\quad (3)$$

The significance Z evaluated on the grid becomes a multivariate Gaussian random vector \hat{Z} with covariance $\hat{\Sigma}$:

$$\hat{Z} \sim \mathcal{N}[\vec{0}, \hat{\Sigma}]. \quad (4)$$

Similarly to the concept of the Asimov data set that may be used to estimate the expected local significance [5], we propose to use a special set of background Asimov data sets to estimate the GP covariance, and subsequently estimate the global significance.

The *set of Asimov data sets* is constructed as follows:

1. Specify the binning of the data (for example invariant mass m) and the grid of scan points for the signal hypothesis (i.e. values for M).
2. Construct the Asimov data set for the background model.
3. For each chosen data bin produce a new data set, where a 1σ upward fluctuation is introduced in that bin of the background Asimov data set (see Sec. 3 for concrete examples).

We assume that the data in different bins are uncorrelated. To construct the approximate covariance, using Eq. 3, we also use the fact that the covariance matrix of a sample of independent measurements can be decomposed into a sum of the partial covariances, in our case calculated from the set of Asimov data sets:

$$\hat{\Sigma} = \sum_i \hat{\Sigma}_i. \quad (5)$$

The final touch is to remember that the diagonal of the constructed covariance is required to be 1. It is not necessarily 1 by our construction, so we

suggest to normalize the $\hat{\Sigma}$:

$$\hat{\Sigma}_{ij} \mapsto \frac{\hat{\Sigma}_{ij}}{\sqrt{\hat{\Sigma}_{ii}\hat{\Sigma}_{jj}}}. \quad (6)$$

By normalizing this way, we again use the assumption that data in the bins are uncorrelated and we also assume that the covariance structure is similar across various scales of fluctuations.

2.1 Number of up-crossings directly from the covariance matrix

Given a differentiable covariance for a Gaussian Process, it is possible to calculate the average number of up-crossings at any level without recourse to any random sampling. This represents a small advancement with respect to the Gross and Vitells extrapolation method.

To motivate the formula in Eq. 11 for the density of up-crossings that we used directly in the form presented by Lutes et al. [6, Example 7.2], we first cite the generic expression for the density $\nu_{X(t)}^+(u)$ of the average number of up-crossings of the level u by any stochastic process $X(t)$ [6, Eq. 7.3]:

$$\nu_X^+(u, t) = p_{X(t)}(u) \int_0^\infty \nu p_{\dot{X}(t)}[\nu \mid X(t) = u] d\nu. \quad (7)$$

In case $X(t)$ is a Gaussian process, meaning $p_{X(t)}$ is a Gaussian density, the distribution of the derivative $\dot{X}(t)$, $p_{\dot{X}(t)}$, follows a Gaussian distribution with mean μ_* and standard deviation σ_* :

$$\begin{aligned}\mu_*(t) &= \frac{K_*(t, t)}{K_{..}(t, t)} u = \rho_*(t, t) \frac{\sigma_*(t)}{\sigma(t)}, \\ \sigma_*(t) &= \sigma_* \sqrt{1 - \rho_*^2(t, t)},\end{aligned}\quad (8)$$

where $\sigma(t) = \sqrt{K(t, t)}$ is the standard deviation of the GP, and μ_* and σ_* are its conditional mean and conditional standard deviation.

The above expressions use a dot notation for derivatives along a single or both axes:

$$K_*(x, y) = \frac{\partial K(x, y)}{\partial y}, \quad K_{..}(x, y) = \frac{\partial^2 K(x, y)}{\partial x \partial y}. \quad (9)$$

Consequently, effective derivatives of the standard deviation and correlation are:

$$\sigma_{\cdot}(t) = \sqrt{K_{\cdot}(t, t)}, \quad \rho_{\cdot}(x, y) = \frac{K_{\cdot}(x, y)}{\sigma_{\cdot}(x)\sigma_{\cdot}(y)}. \quad (10)$$

The expression for the density $\nu(u, t)$ of the average number of up-crossings at the level u by the non-stationary GP with a covariance kernel K and zero mean was derived by Lutes et al. [6, Example 7.2] by integrating explicitly Eq. 7 with the conditional Gaussian distribution $p_{X|Y}$ substituted from Eq. 8 and is:

$$\nu^{+}(u, t) = \frac{e^{\frac{-u^2}{2\sigma^2(t)}}}{\sqrt{2\pi}\sigma(t)} \times \left(\mu_{\star}(t)\Phi\left[\frac{\mu_{\star}(t)}{\sigma_{\star}(t)}\right] + \frac{\sigma_{\star}(t)}{\sqrt{2\pi}}e^{-\frac{\mu_{\star}^2(t)}{2\sigma_{\star}^2(t)}} \right). \quad (11)$$

The analytic results above are valid for a continuous GP kernel. To evaluate these expressions numerically it proved useful to apply 2D spline interpolation to our covariance matrices before computing the derivatives. In this way we managed to reduce the uncertainty introduced by the coarse grid without sacrificing performance much, because spline interpolation provides exact spline derivatives straightforward. We then used Simpson quadrature to integrate the computed density over the mass range.

2.2 Effect of coarse binning on up-crossings

The Gross and Vitells upper bound is based on the average number of up-crossings of some level u by the significance curve $Z(M)$. When computing this number numerically, from MC toys, some finite resolution grid is used to approximate the curve. It turns out that the resolution of the grid affects the resulting number of up-crossings. In this section we investigate this effect on an example of an analytically defined Gaussian process with a squared exponential kernel:

$$K(x, y) = e^{-\frac{(x-y)^2}{\alpha^2}}, \quad \alpha^2 = 10. \quad (12)$$

We generated 1M samples from this GP and counted the average number of up-crossings on a

set of grids with different resolutions. In Fig. 1 we show how the accuracy decreases with the resolution, starting when the bin size exceeds about one third of the correlation length.

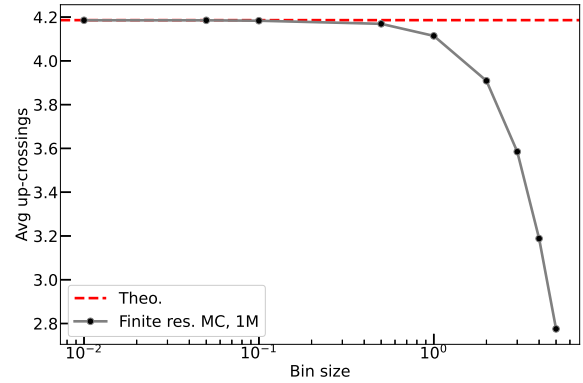


Fig. 1: The average number of up-crossings as a function of bin size. The analytical estimation for the average number of up-crossings (red dashed line) was calculated following Sec. 2.1 for a squared exponential kernel (Eq. 12). The average number of up-crossings for various bin sizes was estimated from 1M GP toys (black dots connected by a gray line). The statistical errors are smaller than the size of the dots.

The underestimation of the number of up-crossings affects the upper bound for the global significance, i.e. the numerator of the trials factor, subsequently the trials factor itself will be underestimated. The local significance, however, which is the denominator, is also affected by the finite grid resolution. The tip of the peak at high significance most probably will appear between grid points, therefore the local significance will also be underestimated.

We investigated the dependency of the effective peak width on its height. We sampled 1M toys from the GP (Eq. 12). For each sample we detected the highest point (x_{max}, y_{max}) , chose a window of 40 around it to select one peak and fitted it with a squared exponential shape $y = A^2 e^{-(x-B)^2/C^2} + D$. For each sample we recorded a pair (y_{max}, C) , where C is the effective peak width. We then removed the failed fit outliers by rejecting the 1% lowest and 1% highest heights. We observed that the average width of the peak decreases with its

height (Fig. 2), therefore, the finite grid effect on the trials factor gains a slight compensation.

In summary, as long as the same grid is used for the data and the analysis of the trials factor, the effect on both will be the same. Consequently, in this study we are not very concerned by the choice of a grid for the signal nuisance parameters, but of course it makes good sense to choose a grid that allows peaks to be described by at least a handful of points.

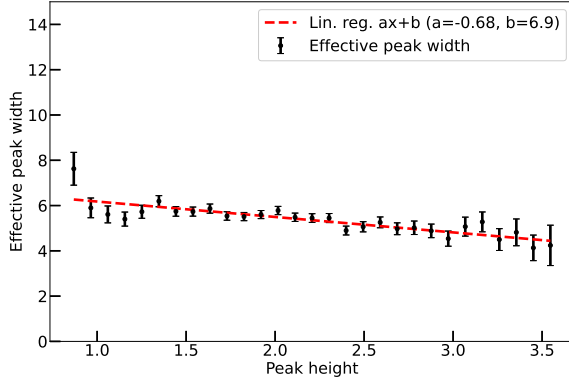


Fig. 2: The average effective width of the highest peak of GP samples for a squared exponential kernel (Eq. 12) as a function of its height for 1M GP toys (black dots) fitted to a linear trend (red dashed line).

3 Examples

The models we use as examples are inspired by searches for new resonances. The invariant masses of signal candidates are binned. Two of the search models have signals with specified widths whereas the third includes the signal width as a free parameter (on a grid) in the likelihood maximization.

3.1 Background template model

Gross and Vitells used this model in their study [1]. It consists of a fixed background shape modeled by the probability density function of the Rayleigh distribution with scale parameter σ_b , and a Gaussian signal with resolution $\sigma_s(M)$ that grows linearly with mass. Background counts D_i are sampled from the Poisson distribution with the rate $b_0 \cdot b_i$ in each bin i of the data grid m_i

defined as follows¹:

$$b_i = N \frac{m_i}{\sigma_b} e^{-\frac{m_i^2}{2\sigma_b^2}}, \quad (13)$$

$$D_i \sim \text{Poisson}[b_0 \cdot b_i],$$

where N was chosen such that $\sum b_i = 1$.

To test the precision of our GP-based approximation of the trials factor we compute the baseline via 10^6 brute force MC simulations of the experiment. We scan each background simulation by testing signal hypotheses for M :

$$s_i(M) = \frac{1}{\sqrt{2\pi}\sigma_s(M)} e^{-\frac{(m_i - M)^2}{2\sigma_s^2(M)}}, \quad (14)$$

$$\sigma_s(M) = A(1 + \frac{M}{B}),$$

and maximize the likelihood with Poisson statistics in the bins of data:

$$N_i = \mu s_i(M) + \beta b_i, \quad (15)$$

$$-\log \mathcal{L}(\mu, M, \beta) = -\sum_i D_i \log(N_i) + \sum_i N_i,$$

where μ and β correspond to the numbers of inferred signal and background events that we vary to maximize the likelihood \mathcal{L} with respect to data D_i , and M is the nuisance parameter that defines the location of the hypothetical signal peak (the constant term of $\log \mathcal{L}$, which plays no role in the maximization, is not shown).

An example of a background simulation and the corresponding significance curve are shown in Fig 3. As a cross-check we compute the average number of up-crossings for the significance threshold of $\sqrt{0.5}$, the same threshold Gross and Vitells used in their work. We get 4.3071 ± 0.0016 up-crossings, which is consistent with their result of 4.34 ± 0.11 .

Next, we generate the set of Asimov background data sets. In this case there are 155 of them, one for each bin of data. One of the Asimov data sets and the corresponding significance curve are shown in Fig 3 for comparison.

For each Asimov data set we compute the partial covariance (see Fig. 4a), then we sum them

¹ $\sigma_b = 40 \text{ GeV}$, $b_0 = 2000$, $A = 2.5 \text{ GeV}$, $B = 50 \text{ GeV}$, $m_i = 0.5 - 154.5 \text{ GeV}$ with a step of 1 GeV , $M_i = 5 - 120 \text{ GeV}$ with a step of 0.25 GeV

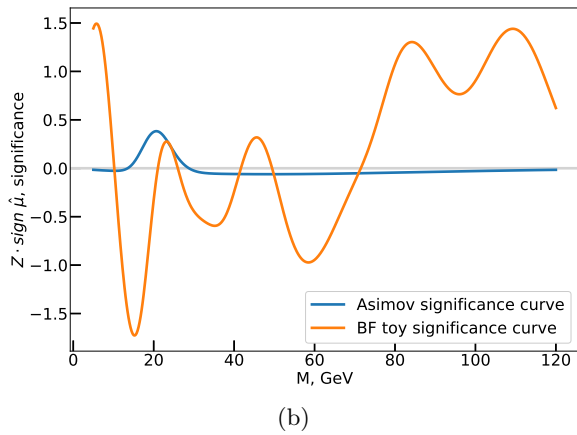
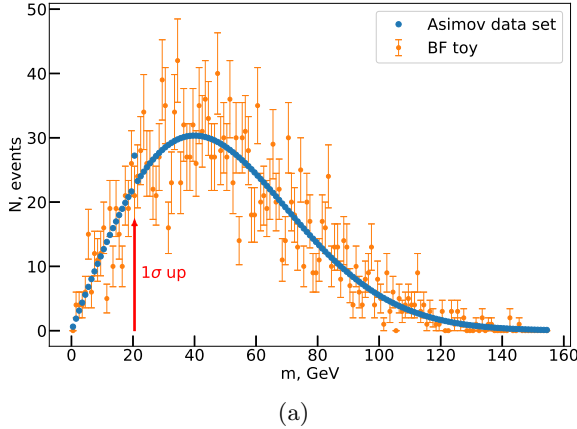


Fig. 3: A background sample, an Asimov toy and the corresponding significance curves from the Background template model. In (a) we show an example of a toy data sampled from the background template (orange dots) and one data set from the set of Asimov data sets (blue dots). The red arrow specifies the bin that was distorted in this particular Asimov data set. In (b) we show the significance curves from the signal plus background fits for the toy sample (orange line) and the Asimov data set (blue line).

and normalize according to Eq. 5 to produce the Asimov GP covariance, shown in Fig. 4b. As expected, the width of the ridge on the diagonal of the covariance matrix is seen to have the same trend as the signal resolution that grows linearly with the mass hypothesis (Eq. 14).

Before using the covariance matrix to sample the significance matrix, let us first evaluate how well we approximate the covariance matrix estimated from the brute force toys. For this we

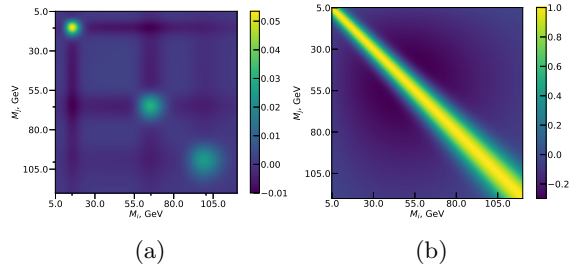


Fig. 4: Partial contributions to the covariance $\hat{\Sigma}(M_i, M_j)$ (a) from 15.5, 65.5 and 100.5 GeV Asimov data sets and the full Asimov GP covariance (b) for the Background template model.

subtract the Asimov covariance, shown in Fig. 4b, from the covariance matrix constructed from 1M brute force toys, shown in Fig. 5a, and plot the difference between the two covariances in Fig. 5b. The differences between Asimov and brute force covariance are 100 times smaller than the values in the covariance itself and for our studies seem to be systematic in nature.

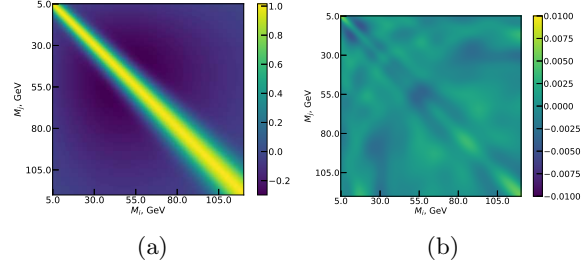


Fig. 5: The difference (b) between the brute force (a) and Asimov (Fig. 4b) covariance matrices calculated for the Background template model.

In our experience, the trials factor appears to be the most sensitive metric to evaluate approximations of the global significance. We estimate the trials factor from $360 \cdot 10^6$ significance curves sampled from the Asimov GP. In Fig. 6 we compare the Asimov GP trials factor, as a function of the local significance, to the brute force approach and approximations that include the Gross and Vitells upper bound and the rule of thumb estimate. The latter was calculated as a ratio of the mass range to the signal resolution, that we average, afterwards, over the mass range, since the resolution changes with the energy scale. We explore the

sensitivity of the TF to the Asimov GP deviations by amplifying the difference between Asimov GP covariance and the brute force covariance by factors of 10 upwards and downwards. From this simple sensitivity analysis we see that visible deviations appear in the very high significance region, in which also the Asimov GP approach is affected by coarse binning effects, and in which the Gross and Vitells upper bound serves as a good approximation to the true TF value. In the same figure we also show that the analytic method described in Sec. 2.1 is in excellent agreement with the Gross and Vitells extrapolated upper bound.

We observe a significant deviation of the Asimov GP from the brute force trials factor estimate at high local significance levels. Qualitatively, we attribute this to the non-gaussianity of the errors introduced by Poissonian statistics that we approximated with a Gaussian distribution. Since the Poisson density is not symmetric around the mean, and is more pronounced for large upward fluctuations, the approximating Gaussian distribution gains upward bias. This effect is smaller at low local significances because the Poisson distribution can be well approximated by a quadratic shape around the mean. We confirmed this by studying the trials factors for larger integrated background rates and observing that the differences at high significance were reduced.

3.2 $H \rightarrow \gamma\gamma$ inspired model

This model is inspired by the ATLAS and CMS searches for the Higgs boson decaying to 2 photons [3, 4]. In this case the background is modeled as an exponential distribution with Gaussian errors σ_b in each bin of data. In order to challenge our method with a more realistic background scenario, in addition to the normalization b_0 , the rate parameter α_b is also unconstrained in the maximum likelihood fits ²:

$$b_i(\alpha_b) = e^{-\frac{(m_i - 100)}{\alpha_b}}, \quad (16)$$

$$D_i \sim \mathcal{N}[b_0 \cdot b_i, \sigma_b].$$

We also simplify the signal model by setting its resolution σ_s to a constant:

$$s_i(M) = \frac{1}{\sqrt{2\pi}\sigma_s} e^{-\frac{(m_i - M)^2}{2\sigma_s^2}}. \quad (17)$$

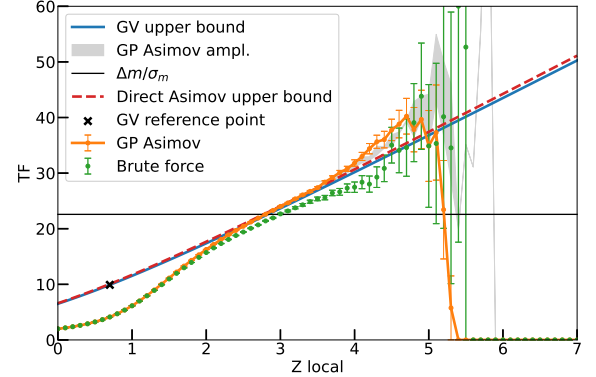


Fig. 6: Trials Factor TF as a function of local significance Z_{local} for the Background template model. We estimated TF from 1M brute force toys (green dots) and compare it to the Asimov GP results (orange line). We color in gray the area enclosed between the two amplified lines from the TF sensitivity study for the Asimov covariance (Sec. 3.1). The solid blue line shows the Gross and Vitells upper bound [1, Eq. 3] extrapolated from the reference significance threshold $\sqrt{0.5}$ (marked by the black cross on the plot). For comparison we show the semi-analytical estimate (Sec. 2.1) of the Gross and Vitells upper bound (red dashed line) and the rule of thumb (black line).

We unify the grids and use the same bins for both sampling of the MC toys (m_i) and signal location scan (M_i). The structure of the likelihood function in this case is:

$$N_i = \mu s_i(M) + \beta b_i(\alpha_b), \quad (18)$$

$$-\log \mathcal{L}(\mu, M, \beta, \alpha_b) = \sum_i (N_i - D_i)^2.$$

Following the same algorithm as for the Gross and Vitells model, we first show an example of the brute force and Asimov background samples (Fig. 7a) together with the corresponding significance curves (Fig. 7b).

Already from the background fit to the Asimov sample (Fig. 7b), we can see that the increased flexibility of the background model introduces more sophisticated long-range correlations. Notice the asymmetry between the left and right sides of the peak. When the signal hypothesis is near the

² $\alpha_b = 0.033 \text{ GeV}$, $b_0 = 10$, $\sigma_b = 0.3 \text{ GeV}$, $\sigma_s = 5 \text{ GeV}$, $m_i = M_i = 100 - 160 \text{ GeV}$ with a step 1 GeV

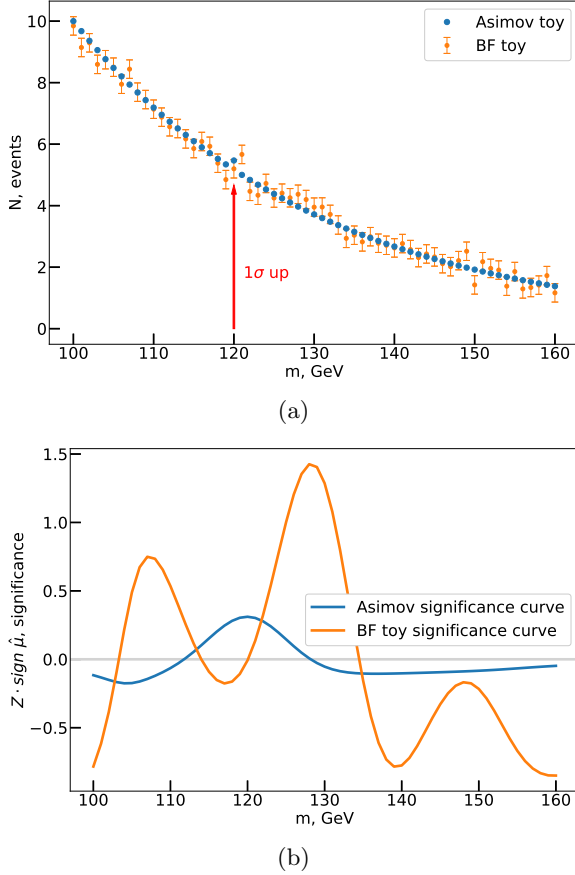


Fig. 7: A background sample, an Asimov toy (a) and the corresponding significance curves (b) from the $H \rightarrow \gamma\gamma$ inspired model. See the detailed explanation of the two plots in Fig. 3.

Asimov fluctuation at 120 GeV, the signal part of the model accommodates it, but well below and above this the rate parameter of the background model tries to compensate for the local excess, which distorts the background model and leads to weak but clear regions of long-range anti-correlation and correlation. We confirm this observation from the plots of the GP covariance that we estimate from the Asimov samples (Fig. 8b).

We then compare the Asimov covariance to the one calculated with brute force (Fig. 9). It shows the same degree of accuracy as we have observed for the Background template model: the differences between the Asimov and brute force covariances are 100 times smaller than the values of the covariance itself.

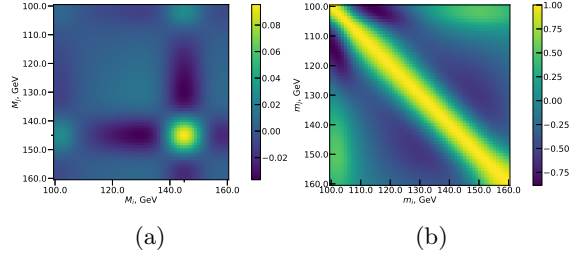


Fig. 8: The partial contribution to the covariance $\hat{\Sigma}(M_i, M_j)$ (a) from the 45.5 GeV Asimov data set and the full Asimov GP covariance (b) for the $H \rightarrow \gamma\gamma$ inspired model.

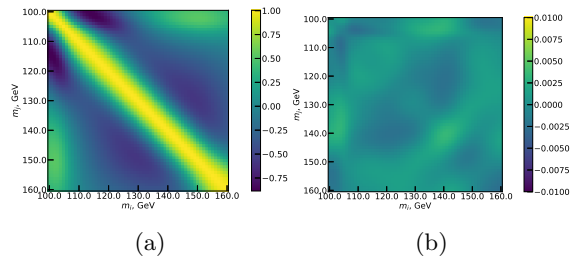


Fig. 9: The difference (b) between the brute force (a) and Asimov (Fig. 8b) covariance matrices calculated for the $H \rightarrow \gamma\gamma$ inspired model.

The various computations of the trials factor for the $H \rightarrow \gamma\gamma$ inspired model are shown in Fig. 10. Since the likelihood and the generation of Monte Carlo data sets both use a Gaussian pdf for the data in each bin, there is no significant difference between the brute force and GP results at high significance, in contrast to the results for the Background template model.

3.3 $H \rightarrow \gamma\gamma$ model with 2-dimensional search region

We keep the background model unchanged from the 1-D example (Eq. 16), however, we want to study a signal model with more than one nuisance parameter. In this case a 1-dimensional significance curve becomes a multidimensional surface. However, each point on this surface still behaves like a standard normal random variable. As defined in Sec. 2, M denotes the set of points that constitute the search region.

For example, in the 2-D case, when in addition to *mass* m_s we also add *width* σ_s as a

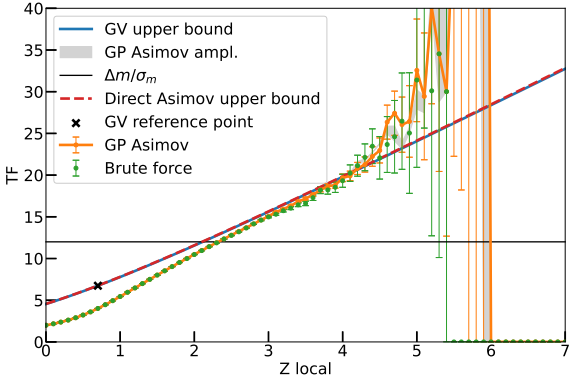


Fig. 10: Trials Factor TF as a function of local significance Z_{local} for the $H \rightarrow \gamma\gamma$ inspired model. See the detailed explanation of the plot in Fig. 6.

second nuisance parameter, M gains a second axis, consequently, the significance surface becomes 2-dimensional. The signal model for this example is³

$$s_i(M) = s_i(m_s, \sigma_s) = \frac{1}{\sqrt{2\pi}\sigma_s} e^{-\frac{(m_i - m_s)^2}{2\sigma_s^2}}. \quad (19)$$

The likelihood function is the same as for the 1-D case (see Eq. 18).

For the covariance calculation the situation does not change if we think in terms of M , i.e., the expressions in Eq. 3 still hold. For visualization, on the contrary, it is convenient to distinguish between *mass* and *width* dimensions. The transition between M_{mn} , that preserves *mass* and *width* correspondingly, and M_i can be constructed as follows:

$$\{M_1, M_2, \dots\} \quad (20)$$

↓

$$\{M_{11}, \dots, M_{1k}, M_{21}, \dots, M_{2k}, M_{31}, \dots\}.$$

In Fig. 11 we visualize the Asimov covariance matrix in the 2-dimensional case, which we unwrapped according to Eq. 20. We also show different projections of this covariance and compare the Asimov covariance to the brute force covariance computed with 3M toys in Fig. 12. We again observe that the differences between covariances

³ $\alpha_b = 0.033 \text{ GeV}$, $b_0 = 10$, $\sigma_b = 0.3 \text{ GeV}$, $M_{ij} = (a_i, b_j)$, $m_i = 100 - 160 \text{ GeV}$ with a step of 1 GeV; $a_i = 100 - 160 \text{ GeV}$ and $b_i = 1 - 10 \text{ GeV}$ with 61 points on the grid each.

(Fig. 12e) are 100 times smaller than the values in the covariance matrix in Fig. 11.

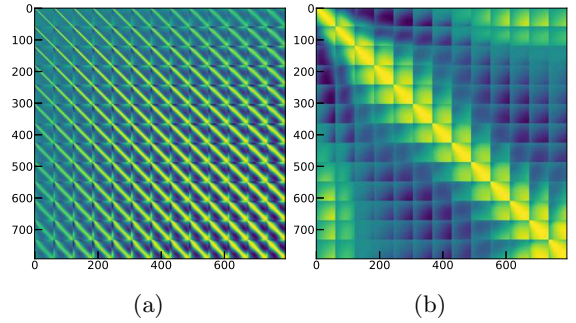


Fig. 11: 4D covariance matrix unwrapped into 2D following Eq. 20 (a) and its transposed version (b), for the $H \rightarrow \gamma\gamma$ inspired model with a 2D search region. For the purpose of illustration, the less frequently changing dimension on each plot has a reduced number of points, consequently, the plots have a reduced number of “squares”.

The trials factors we obtained for this model are shown in Fig. 13. In this case the Vitells and Gross upper bound [2] is based on the Euler characteristic of the 2-dimensional significance surface. The upper bound calculation requires the Euler characteristic to be known at two significance levels (black crosses) before extrapolation. From the qualitative comparison of Fig. 13 to Fig. 6 and Fig. 10 it seems that for a higher dimensional search region, the Vitells and Gross upper bound becomes even more conservative.

4 Conclusion

A precise estimation of the look-elsewhere effect in searches for new resonances in high energy physics is challenging. Existing methods are overly conservative unless the observed local significance is high enough. In this paper we proposed and evaluated a new approach based on Gaussian processes. The new approach doesn't eliminate the production of many Monte Carlo “toys”, however, the computational process becomes much more efficient. We tested the approach on several models, including models with more than 1 nuisance parameter, that intentionally were constructed to have different statistical features. The trials factors calculated with our new approach and with large samples

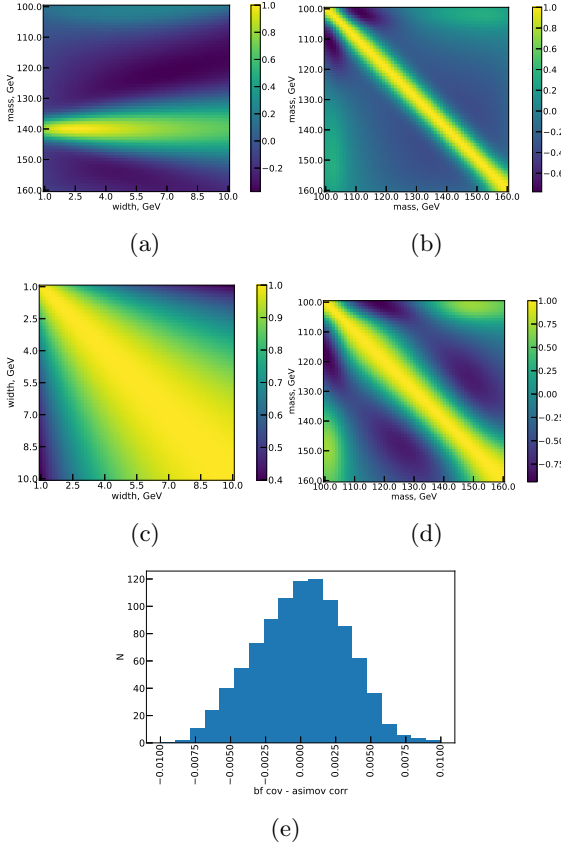


Fig. 12: Covariance for the 2D $H \rightarrow \gamma\gamma$ model (in the 2D case a covariance between two significance surfaces). The covariance between the point on the first surface and 1 chosen point of mass and width ($m_s = 140$ GeV, $\sigma_s = 2.5$ GeV) from the second surface is shown in (a). The covariance between the slices of surfaces, where σ_s was fixed for both surfaces, is shown in (b) for $\sigma_s = 3.25$ GeV and in (d) for $\sigma_s = 7$ GeV. Similarly, (c) shows the pattern for the slices where m_s is set to 130 GeV for both surfaces. A histogram of the differences between the elements of the Asimov and brute force covariance matrices is shown in (e).

of brute force Monte Carlo simulations showed excellent agreement. As a cross-check, we reproduced the result of the Gross and Vitells paper [1] that introduced the high-significance approximation based on up-crossings. An actual realization of the method and implementation of the test models was published and is available for use out of the box [7].

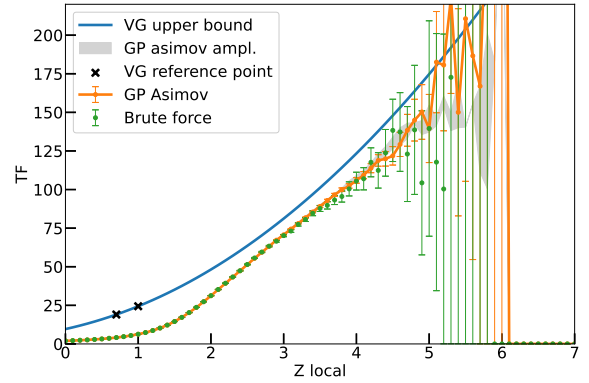


Fig. 13: Trials Factor TF as a function of local significance Z_{local} for the $H \rightarrow \gamma\gamma$ inspired model with 2D search region. The green dots, orange line, and gray area are explained in Fig.6. The solid blue line shows the Vitells and Gross upper bound [2] extrapolated from the two reference significance thresholds ($\sqrt{0.5}$ and 1) (black crosses).

Acknowledgments. We would like to thank Ofer Vitells for several very helpful discussions, in particular about the details of the statistical model in the Gross and Vitells paper. This research was supported by the European Union Framework Programme for Research and Innovation Horizon 2020 (2014–2021) under the Marie Skłodowska-Curie Grant Agreement No.765710.

References

- [1] Gross, E., Vitells, O.: Trial factors for the look elsewhere effect in high energy physics. *The European Physical Journal C* **70**(1-2), 525–530 (2010). <https://doi.org/10.1140/epjc/s10052-010-1470-8>
- [2] Vitells, O., Gross, E.: Estimating the significance of a signal in a multi-dimensional search. *Astroparticle Physics* **35**(5), 230–234 (2011). <https://doi.org/10.1016/j.astropartphys.2011.08.005>
- [3] ATLAS Collaboration: Search for the standard model higgs boson in the diphoton decay channel with 4.9 fb^{-1} of pp collision data at $\sqrt{s} = 7$ TeV with atlas. *Phys. Rev. Lett.* **108**, 111803 (2012). <https://doi.org/10.1103/PhysRevLett.108.111803>

- [4] CMS Collaboration: Search for the standard model higgs boson decaying into two photons in pp collisions at $\sqrt{s} = 7 \text{ TeV}$. Physics Letters B **710**(3), 403–425 (2012). <https://doi.org/10.1016/j.physletb.2012.03.003>
- [5] Cowan, G., Cranmer, K., Gross, E., Vitells, O.: Asymptotic formulae for likelihood-based tests of new physics. The European Physical Journal C **71**(2) (2011). <https://doi.org/10.1140/epjc/s10052-011-1554-0>
- [6] Lutes, L.D., Sarkani, S.: Random Vibrations. Analysis of Structural and Mechanical Systems. Butterworth Heinemann, Boston (2004)
- [7] Ananyev, V., Read, A.: Repository containing the source code of the Gaussian process based approach with examples. (2022). <https://gitlab.cern.ch/ananyev/sigcorr>